

# Supporting information

---

## Contents

1. Asymptotic solutions.....	2
1.1 Formation of asymptotic limits .....	2
1.2 Infinitely stiff spring limit .....	3
1.3 Determination of the viscoelastic parameters in the asymptotic limit .....	4
1.4 References .....	4
2. Numerical solution.....	4
2.1: NAG library algorithm D05BA .....	4
2.2: Alternative numerical solver .....	5
2.3: Trapezoidal rule .....	5
2.4: Implementation .....	5
2.5: Ramp phase.....	6
2.6: Hold phase .....	7
2.7: Stability: .....	7
2.8: Exploration of polynomial.....	8
3. Errors.....	9
4. Master curves for $E_{\infty}^*$ .....	10
4.1 Variations in $G_1$ and $G_2$ follow a simple rule between them and the optimal spring stiffness:.....	10
4.2 Variations in $\tau$ :.....	11
4.3 Variations in $\gamma$ :.....	12
4.4 Master curve for $h^*$ :.....	13
5. Linear programming.....	15
5.1: Linear programming for optimisation of parameters:.....	15
5.2: Maximum relative relaxation.....	15
5.3: Linear programming construction .....	16
5.4 References .....	16
6. Construction of permissible indentation region .....	16
6.1: Physical limits.....	17
6.2: Calibration of spring constant axis.....	18
6.3: Possible experimental region.....	19

6.4: Lines of constant force.....	19
6.5: Signal to noise limit.....	20
6.6: Typical experimental situation:.....	21
7. Poroelasticity .....	21
7.1 References .....	23
8. Physical models and an equivalent viscoelastic material .....	23

## 1. Asymptotic solutions

The asymptotic approach detailed here is of particular interest when the cantilever is stiff or the ramp duration is short. Many useful results may be determined and these are found in this section.

### 1.1 Formation of asymptotic limits

Few analytic solutions of non-linear Volterra equations are known,<sup>1</sup> to progress further equation (6) in the manuscript is linearised by assuming  $Ak/G_1 \gg h^{1/2}(x)$  for all  $x$  in the interval  $[0, t]$ , this is exact in the limit as  $k \rightarrow \infty$ , i.e. infinite spring stiffness,

$$h_0(t) = \begin{cases} f_1(t) - \lambda \int_0^t h_0(\xi) e^{-\frac{\xi-t}{\tau}} d\xi : 0 \leq t \leq \gamma & \text{Ramp phase} \\ f_2(t) - \lambda \int_0^t h_0(\xi) e^{-\frac{\xi-t}{\tau}} d\xi : t > \gamma & \text{Hold phase} \end{cases} \quad (1.1)$$

where  $h_0(t)$  is the indentation depth in this limit,  $\lambda = \mu/\tau$ ,

$$f_1(t) = (1 + \mu)(Vt + h(0)) - \mu V \tau \left(1 - e^{-\frac{t}{\tau}}\right) - \mu h(0) e^{-\frac{t}{\tau}}$$

$$\text{and } f_2(t) = (1 + \mu)(V\gamma + h(0)) - \mu V \tau \left(e^{-\frac{\gamma-t}{\tau}} - e^{-\frac{t}{\tau}}\right) - \mu h(0) e^{-\frac{t}{\tau}}.$$

Equation (1.1) is a linear Volterra equation of the second kind and has the following exact solution,

$$h_0(t) = \begin{cases} Vt + h(0) & : 0 \leq t \leq \gamma, \\ V\gamma + h(0) & : t > \gamma. \end{cases} \quad (1.2)$$

To investigate corrections to this linear limit consider  $h(t) = h_0(t) + E(t)$ , where  $E(t)$  is the correction to the infinite spring stiffness solution, combined with equation (4) in the manuscript and equation (1.1), defining  $\chi = G_1/(Ak)$ , the following is obtained,

$$E(t) + \chi(h_0(t) + E(t))^{3/2} = -\lambda \int_0^t E(\xi) e^{\frac{\xi-t}{\tau}} d\xi, \quad (1.3)$$

this is another non-linear Volterra equation of the second kind and may be linearised by expanding  $(h_0(t) + E(t))^{3/2} = h_0^{3/2}(t)(1 + 3E(t)/(2h_0(t)) + O((E(t)/h_0(t))^2))$ . Substituting the first term,  $h_0^{3/2}(t)$ , into equation (6) in the manuscript produces the following linear Volterra equation of the second kind,

$$E_1(t) = \begin{cases} -\chi h_0^{3/2}(t) - \lambda \int_0^t E_1(\xi) e^{\frac{\xi-t}{\tau}} d\xi : 0 \leq t \leq \gamma & \text{Ramp phase} \\ -\chi h_0^{3/2}(t) - \lambda \int_0^t E_1(\xi) e^{\frac{\xi-t}{\tau}} d\xi : t > \gamma & \text{Hold phase.} \end{cases} \quad (1.4)$$

where  $E_1(t)$  is the leading order solution of equation (1.3). The solution to this linear Volterra equation of the second kind is,

$$E_1(t) = \begin{cases} -\chi(V)^{3/2} \left( t^{3/2} - \frac{\lambda}{4\kappa^{5/2}} e^{-\kappa t} (3\sqrt{\pi} \operatorname{erfi}(\sqrt{\kappa t}) + 2\sqrt{\kappa t} e^{\kappa t} (2\kappa t - 3)) \right) & : 0 \leq t \leq \gamma \quad \text{Ramp phase} \\ -\chi(V\gamma)^{3/2} \left( \frac{1}{\tau\kappa} - \frac{\lambda}{4\kappa^{5/2}\gamma^{3/2}} e^{-\kappa t} (3\sqrt{\pi} \operatorname{erfi}(\sqrt{\kappa\gamma}) + 2\sqrt{\kappa\gamma} e^{\kappa\gamma} (2\kappa\gamma - 3)) + e^{\kappa(\gamma-t)} \left( 1 - \frac{1}{\tau\kappa} \right) \right) & : t > \gamma \quad \text{Hold phase} \end{cases} \quad (1.5)$$

where  $\kappa = (1 + \mu)/\tau$  and  $E(t)/h_0(t) \ll 1$ .

## 1.2 Infinitely stiff spring limit

When the cantilever stiffness is infinite, controlling the position of the fixed end is equivalent to controlling the position of the spherical indenter, as demonstrated by equation (1.2). When equation (1.2) is substituted into equation (2) in the manuscript, this produces a force (0 N) which is in direct violation of Lee and Radok<sup>2</sup> result for controlling the position of the spherical indenter for a Maxwell fluid during the ramp phase. This apparent paradox is resolved by noting that equation (1.5) contributes to the force even as  $k \rightarrow \infty$  and substituting this produces the following equation,

$$F(t) = \begin{cases} \frac{G_1}{A} (V)^{3/2} \left( t^{3/2} - \frac{\lambda}{4\kappa^{5/2}} e^{-\kappa t} (3\sqrt{\pi} \operatorname{erfi}(\sqrt{\kappa t}) + 2\sqrt{\kappa t} e^{\kappa t} (2\kappa t - 3)) \right) & : 0 \leq t \leq \gamma \quad \text{RP} \\ \frac{G_1}{A} (V\gamma)^{3/2} \left( \frac{1}{\tau\kappa} - \frac{\lambda}{4\kappa^{5/2}\gamma^{3/2}} e^{-\kappa t} (3\sqrt{\pi} \operatorname{erfi}(\sqrt{\kappa\gamma}) + 2\sqrt{\kappa\gamma} e^{\kappa\gamma} (2\kappa\gamma - 3)) + e^{\kappa(\gamma-t)} \left( 1 - \frac{1}{\tau\kappa} \right) \right) & : t > \gamma \quad \text{HP} \end{cases} \quad (1.6)$$

Furthermore, this solution corresponds to the force provided by Lee and Radok<sup>2</sup> when  $G_2 = 0$ . The hold phase was not considered by Lee and Radok<sup>2</sup> for the controlled position case, also equation (1.6) includes the corrections to the force due to a large but finite stiffness of the cantilever (i.e.  $\Phi \gg 1$ ), since the derivation differs significantly here from Lee and Radok,<sup>2</sup> agreement indicates that this model is consistent and has the correct limits as  $k \rightarrow \infty$ .

### 1.3 Determination of the viscoelastic parameters in the asymptotic limit

Although it is possible to determine the three viscoelastic parameters by fitting the force to equation (1.6), this is likely to produce significant errors. Instead, the ramp phase from equations (1.2) and (1.5) may be considered for short durations; should  $G_1(V\gamma)^{1/2}/(Ak) \ll 1$  then  $E(t)/h_0(t) \ll 1$  is automatically satisfied. In this case the force is approximated by,

$$F \approx \frac{G_1 V^{3/2} t^{1/2}}{A} \left( 1 - \frac{2\lambda t}{5} + \frac{2\lambda \kappa t^2}{105} \right). \quad (1.7)$$

Equation (1.7) can be used to determine  $G_1$ . To determine the value of  $G_2$ , consider the hold phase. Taking the limit  $\hat{E}_\infty = \lim_{t \rightarrow \infty} E(t)$ , the following result is obtained

$\hat{E}_\infty = -G_1 G_2 (V\gamma)^{3/2} / (Ak(G_1 + G_2))$ . When  $G_2 \sim G_1$  or  $G_2 \ll G_1$  this approach will give reasonable estimates for  $G_2$ . As  $G_2 \rightarrow \infty$ ,  $\hat{E}_\infty = -G_1 (V\gamma)^{3/2} / (Ak)$  no further information may be obtained from this limit. Alternatively, during the hold phase the following equation is valid,

$$1 - \frac{E_1(t)}{E_\infty} = \lambda \omega e^{-\kappa t} \quad (1.8)$$

with  $\omega = \left( e^{\kappa \gamma} 2\sqrt{\kappa \gamma} (2\gamma \kappa - 3) + \sqrt{3\pi} \operatorname{erfi}(\sqrt{\kappa \gamma}) \right) / 4\kappa^{3/2} \gamma^{3/2} + e^{\kappa(\gamma-t)} (\kappa - 1)$ , hence  $\lambda$  and  $\kappa$  can be determined; from these the parameters  $G_2$  and  $\tau$  to be determined as follows,  $\tau = 1/(\kappa - \lambda)$  and  $G_2 = G_1(\kappa - \lambda) / \lambda$ .

### 1.4 References

- 1 P. Linz, *Analytical and numerical methods for Volterra equations*, SIAM, 1985, ch. 1, pp 3-4.
- 2 E. H. Lee and J. R. M. Radok, *Journal of Applied Mechanics*, 1968, **27**, 438-444.

## 2. Numerical solution

The two numerical solutions discussed in this section can be split simply into, an efficient solver using an algorithm developed by NAG and a licence must be acquired for use. However typically a simpler algorithm may be invoked but greater computational effort is required, this second approach is discussed in detail so that a simple and usable code may be developed without access to a numerical algorithm licence.

### 2.1: NAG library algorithm D05BA

The solutions presented in §1 are approximate. To confirm their limits a numerical procedure has been developed to solve equation (6) in the manuscript directly, by evaluating the integral using the NAG library algorithm D05BA. This algorithm requires the Volterra equation to be written in standard form with

$$\Sigma(t) = h(t) \left( \frac{Ak}{G_1} + h^{1/2}(t) \right)$$

$$\varphi = \left( 108\Sigma(t) - 8 \left( \frac{Ak}{G_1} \right)^3 + 12 \sqrt{3\Sigma(t) \left( 27\Sigma(t) - 4 \left( \frac{Ak}{G_1} \right)^3 \right)} \right)^{1/3}$$

and the standard form is,

$$\Sigma(t) = a(t) - \alpha \int_0^t \frac{\left( \varphi^2(\xi) + 4 \left( \frac{Ak}{G_1} \right)^2 - 2 \left( \frac{Ak}{G_1} \right) \varphi(\xi) \right)}{36\varphi^2(\xi)} e^{(\xi-t)/\tau} d\xi$$

where  $a(t) = a_1(t)$  [equation (6a) in the manuscript] or  $a(t) = a_2(t)$  [equation (6b) in the manuscript] as appropriate and the solution for  $h(t)$  requires the solution of the polynomial defining  $\Sigma(t)$ . D05BA requires the integrand and the function  $a(t)$  to be provided  $x$  as inputs, and  $\Sigma(t)$  is returned; an example is provided in the NAG library documentation and involves replacing the integrand and the function with the equations detailed above to obtain this algorithm. Since the NAG routine requires a licence for the NAG library an alternative is provided in the supporting information, however greater computational effort is required to obtain satisfactory results.

## 2.2: Alternative numerical solver

The numerical solver discussed in the manuscript requires access to the NAG routines. A simpler code will be described here which can be written using most programming languages, however a Matlab® code is supplied illustrating its implementation.

## 2.3: Trapezoidal rule

The integration needs to be evaluated and the indentation depth solved. The first step requires a numerical scheme to perform the integration; the trapezoidal rule (on a uniform grid) is implemented in this case,

$$\int_a^b f(x) dx \approx \tilde{h} \sum_{k=1}^N (f(x_{k+1}) - f(x_k)) = \frac{b-a}{2N} (f(x_1) + 2f(x_2) + 2f(x_3) + \dots + 2f(x_N) + f(x_{N+1}))$$

where the domain of integration is discretised into  $N$  equally spaced grid points, of grid spacing  $\tilde{h} = (b-a)/N$ .

## 2.4: Implementation

The full nonlinear Volterra equation may be found in the manuscript in equations (6), (6a) and (6b) and are reproduced here,

$$h(t) \left( \frac{Ak}{G_1} + h^{1/2}(t) \right) = \begin{cases} a_1(t) - \alpha \int_0^t h(\xi) e^{\frac{\xi-t}{\tau}} d\xi: & 0 \leq t \leq \gamma \text{ Ramp Phase} \\ a_2(t) - \alpha \int_0^t h(\xi) e^{\frac{\xi-t}{\tau}} d\xi: & t > \gamma \text{ HoldPhase} \end{cases} \quad (2.1)$$

where  $\alpha = Ak/G_1$ ,

$$a_1(t) = Ak \left( \frac{1}{G_1} + \frac{1}{G_2} \right) (Vt + h(0)) - \frac{AkV\tau}{G_2} \left( 1 - e^{-\frac{t}{\tau}} \right) - \frac{Akh(0)}{G_2} e^{-\frac{t}{\tau}} \quad (2.1a)$$

$$a_2(t) = Ak \left( \frac{1}{G_1} + \frac{1}{G_2} \right) (V\gamma + h(0)) - \frac{AkV\tau}{G_2} \left( e^{\frac{\gamma-t}{\tau}} - e^{-\frac{t}{\tau}} \right) - \frac{Akh(0)}{G_2} e^{-\frac{t}{\tau}}. \quad (2.1b)$$

To solve equation (2.1) the trapezoidal rule is applied at each time step to determine a polynomial which enables the indentation depth at the next time step to be determined.

### 2.5: Ramp phase

The problem is naturally split into two, the ramp phase and the hold phase here the ramp phase will be considered in depth. As a simple example consider the first step,  $t = \tilde{h}$ ,  $h(0) = 0$ ,

$$h(\tilde{h}) \left( \frac{Ak}{G_1} + h^{1/2}(\tilde{h}) \right) = a_1(\tilde{h}) - \alpha \int_0^{\tilde{h}} h(\xi) e^{\frac{\xi-\tilde{h}}{\tau}} d\xi \approx a_1(\tilde{h}) - \alpha \left\{ \frac{\tilde{h}}{2} \left[ h(0) \exp\left(\frac{-\tilde{h}}{\tau}\right) + h(\tilde{h}) \right] \right\} \quad (2.2)$$

collecting all the terms on the left hand side (LHS) depending on  $h(\tilde{h})$  and substituting  $g(t) = h^{1/2}(t)$ , the following is obtained,

$$g^2(\tilde{h}) \left( \frac{Ak}{G_1} + \frac{\alpha\tilde{h}}{2} + g(\tilde{h}) \right) = a_1(\tilde{h}) - \frac{\alpha\tilde{h}}{2} \left( g^2(0) \exp\left(\frac{-\tilde{h}}{\tau}\right) \right). \quad (2.3)$$

The solution to the polynomial in equation (2.3) enables the indentation depth to be obtained from,  $h(t) = g^2(t)$ . Equation (2.3) may be generalised for any number of  $\tilde{h}$  increments as the following equation,  $t \leq \gamma$

$$g^2(t) \left( \frac{Ak}{G_1} + \frac{\alpha\tilde{h}}{2} + g(t) \right) = a_1(t) - \alpha I - \frac{\alpha\tilde{h}}{2} \left( g^2(t - \tilde{h}) \exp\left(\frac{-\tilde{h}}{\tau}\right) \right) \quad (2.4)$$

where  $I = \int_0^{t-\tilde{h}} h(\xi) e^{\frac{\xi-t}{\tau}} d\xi$ , obtained by the trapezoidal rule. Writing the LHS of equation (2.4) as,

$$g^2(t) \left( \frac{Ak}{G_1} + \frac{\alpha\tilde{h}}{2} + g(t) \right) = g^2(t) (L + g(t)) \quad (2.5)$$

with  $L = Ak/G_1 + \alpha\tilde{h}/2$  and the right hand side of equation (RHS) (2.4),

$$\varpi_1 = a_1(t) - \alpha I - \frac{\alpha\tilde{h}}{2} \left( g^2(t - \tilde{h}) \exp\left(\frac{-\tilde{h}}{\tau}\right) \right). \quad (2.6)$$

The solution to equation (2.4) may now be expressed as,

$$\psi_1 = \left( 108\varpi_1 - 8L^3 + 12\sqrt{81\varpi_1^2 - 12\varpi_1L^3} \right)^{1/3} \quad (2.7)$$

$$g(t) = \frac{\psi_1}{6} + \frac{2L^2}{3\psi_1} - \frac{L}{3}. \quad (2.8)$$

## 2.6: Hold phase

The hold phase is very similar to the ramp phase except  $a_1(t)$  is replaced by  $a_2(t)$  and the preceding integral,  $I_\gamma = \int_0^\gamma h(\xi)e^{\frac{\xi}{\tau}} d\xi$  is required from the hold phase. For the first time step of the hold phase,  $t = \gamma + \tilde{h}$ , the indentation depth at the end of the ramp duration is required,  $h(\gamma)$ , from the ramp phase. The appropriate version of equation (2.4) for the hold phase is,  $t > \gamma$

$$g^2(t) \left( \frac{Ak}{G_1} + \frac{\alpha\tilde{h}}{2} + g(t) \right) = a_2(t) - \alpha I - \frac{\alpha\tilde{h}}{2} \left( g^2(t - \tilde{h}) \exp\left(\frac{-\tilde{h}}{\tau}\right) \right) \quad (2.9)$$

where  $I = \int_0^{\tilde{h}} h(\xi)e^{\frac{\xi-t}{\tau}} d\xi = e^{-\frac{t}{\tau}} I_\gamma + \int_\gamma^{\tilde{h}} h(\xi)e^{\frac{\xi-t}{\tau}} d\xi$ . It should be noted that evaluation of

$I_t = \int_0^t h(\xi)e^{\frac{\xi}{\tau}} d\xi$  represents efficient storage of the integral and multiplying by  $e^{-\frac{t}{\tau}}$  modifies the results to the appropriate form. Writing the LHS of equation (2.9) as,

$$g^2(t) \left( \frac{Ak}{G_1} + \frac{\alpha\tilde{h}}{2} + g(t) \right) = g^2(t)(L + g(t)) \quad (2.10)$$

with  $L = Ak/G_1 + \alpha\tilde{h}/2$  and the right hand side of equation (RHS) (2.9),

$$\varpi_2 = a_2(t) - \alpha I - \frac{\alpha\tilde{h}}{2} \left( g^2(t - \tilde{h}) \exp\left(\frac{-\tilde{h}}{\tau}\right) \right). \quad (2.11)$$

The solution to equation (2.9) may now be expressed as,

$$\psi_2 = \left( 108\varpi_2 - 8L^3 + 12\sqrt{81\varpi_2^2 - 12\varpi_2L^3} \right)^{1/3} \quad (2.12)$$

$$g(t) = \frac{\psi_2}{6} + \frac{2L^2}{3\psi_2} - \frac{L}{3}. \quad (2.13)$$

## 2.7: Stability:

The stability of the numerical solver is governed by the standard stability parameter for an iterative solve assume,

$$g_{i+1} = f(g_i) \quad (2.14)$$

the square root of the indentation depth at the next time step,  $g_{i+1}$ , may be expressed as a function of the square root of the indentation depth at the  $i^{\text{th}}$  time step,  $g_i$ . The stability criterion may be determined as,  $\lambda = \frac{\partial g_{i+1}}{\partial g_i}$  and  $|\lambda| < 1$  for stability. Differentiating equation (2.4) with respect to  $g_i$  and rearranging to find  $\lambda$ ,

$$\lambda = \frac{2Ak\tilde{h}g_i e^{-\tilde{h}/\tau}}{G_2\tau g_{i+1}(3g_{i+1} + 2L)}. \quad (2.15)$$

Equation (2.15) will always be satisfied if  $\tilde{h}$  is large enough however the local truncation error of this code depends on  $O(\tilde{h}^2)$  and hence the time step,  $\tilde{h}$ , can't be arbitrarily large. During the ramp phase there are two extreme limits which can be considered easily,

- i) The spring stiffness is infinite,  $k \rightarrow \infty$ . The position of the indenter is directly controlled and  $g_i = \kappa$  and  $g_{i+1} = \kappa + V\tilde{h}$ ,

$$\lambda = \frac{2Ak\tilde{h}e^{-\tilde{h}/\tau}}{G_2\tau\left(1 + \frac{V\tilde{h}}{\kappa}\right)\left(3(\kappa + V\tilde{h}) + 2L\right)} \quad (2.16)$$

$$\lim_{k \rightarrow \infty} \lambda = \frac{2\tilde{h}e^{-\tilde{h}/\tau}}{\tau\left(1 + \frac{V\tilde{h}}{\kappa}\right)\left[\frac{2G_2}{G_1} + \frac{\tilde{h}}{\tau}\right]} \quad (2.17)$$

Equation (2.17) ensures that it is always possible to obtain a stable time step, since as  $k \rightarrow \infty$ ,  $\lambda$  is finite, and hence a finite  $\tilde{h}$  can be determined.

- ii) The spring is perfectly compliant,  $k = 0$ . The position of the indenter remains the same for all time,  $g_i = \kappa$  and  $g_{i+1} = \kappa$ ,

$$\lambda = \frac{2Ak\tilde{h}e^{-\tilde{h}/\tau}}{G_2\tau(3\kappa + 2L)} \quad (2.18)$$

$$\lim_{k \rightarrow 0} \lambda = 0 \quad (2.19)$$

Equation (2.19) ensures that for a perfectly compliant spring the code is absolutely convergent.

Cases i) and ii) represent extreme cases and since by careful selection of the time step,  $\tilde{h}$ , it is possible to obtain a stable numerical scheme in both cases; all cases can be stabilised by appropriate choice of the time step.

## 2.8: Exploration of polynomial

Equations (2.1), (2.4) and (2.9) have a similar form which allows for a simple representation of the polynomial. Writing these polynomials as,

$$g(t)^2(L + g(t)) = RHS \quad (2.20)$$

where  $RHS$  is the appropriate right hand side of equations (2.1), (2.4) and (2.9) and is a monotonically increasing function of  $t$ ;  $L$  is  $Ak/G_1$  for equation (1) and  $Ak/G_1 + \alpha\tilde{h}/2$  for equations (2.4) and (2.9). A plot of equation (2.20) against  $g(t)$  in figure 2.1, provides a simple and direct visualisation of the solution procedure implemented here and in the manuscript. The maximum indentation depth possible is  $V\gamma$  and this imposes a limit on the maximum value of  $RHS$ .

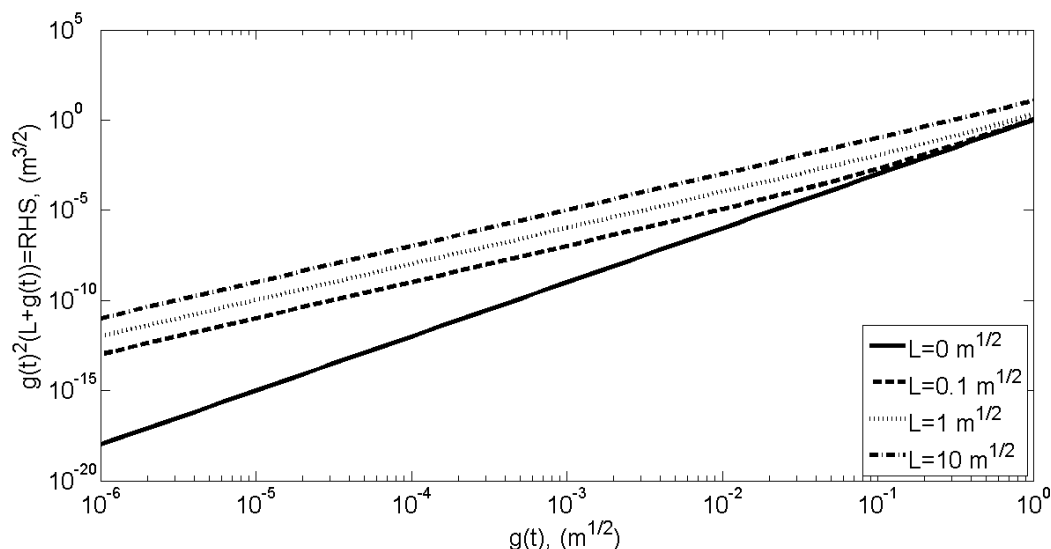


Figure 2.1: Polynomial to determine the square root of the indentation depth plotted for different constants  $L$ , as the  $RHS$  increases the indentation depth also increases

### 3. Errors

The errors in the indentation affect the errors in the force, the equation relating the two has been supplied in the manuscript equation (9). However the equation is quite general and may be used to determine if a force or indentation depth relaxation is appropriate,

$$h'(t) = h(t) + u(t),$$

where  $h(t)$  is the actual indentation depth,  $u(t)$  is the error in the indentation depth and  $h'(t)$  is the measured indentation depth. The relative error in the indentation depth is then,

$$\mathfrak{R} = \frac{|h(t) - h'(t)|}{h(t)}.$$

The relative error in the force measurement given the known indentation depth is supplied by,

$$\mathfrak{S} = \frac{|F - F'|}{F} = \begin{cases} \frac{|k(Vt - h(t)) - k(Vt - h'(t))|}{k(Vt - h(t))} = \frac{|h(t) - h'(t)|}{(Vt - h(t))} = \frac{|h(t) - h'(t)|/(Vt)}{(1 - h(t)/(Vt))} = \frac{h(t)R/(Vt)}{(1 - h(t)/(Vt))} & \text{for } t \leq \gamma \\ \frac{|k(V\gamma - h(t)) - k(V\gamma - h'(t))|}{k(V\gamma - h(t))} = \frac{|h(t) - h'(t)|}{(V\gamma - h(t))} = \frac{|h(t) - h'(t)|/(V\gamma)}{(1 - h(t)/(V\gamma))} = \frac{h(t)R/(V\gamma)}{(1 - h(t)/(V\gamma))} & \text{for } t > \gamma \end{cases}$$

where  $F$  is the actual force and  $F'$  is the measured force. Since any real experiment is prone to errors these relative errors enable selection of the appropriate test to ensure that the desired results have minimum error. Stiff systems benefit from determination of the indentation depth over the force as  $(1 - h(t)/(Vt))$  tends to zero and hence small errors in the force result in large errors in the measured force curves. Similarly highly compliant systems tend to benefit from the determination of the force over the indentation depth as  $h$  tends to zero. It is interesting to note that the optimal indentation conditions typically hover around the force and indentation criteria being equivalent and hence it makes little difference which is measured at optimum. However as the force is typically a derived quantity the indentation depth is preferred.

#### 4. Master curves for $E_{\infty}^*$

There are two master curves that are essential to the work presented in the manuscript, effectively these curves provide the two parameters  $E_{\infty}^*$  and  $h^*$  for a vast range of materials and system parameters. The generation of the equations and hence the master curves is detailed briefly here.

##### 4.1 Variations in $G_1$ and $G_2$ follow a simple rule between them and the optimal spring stiffness:

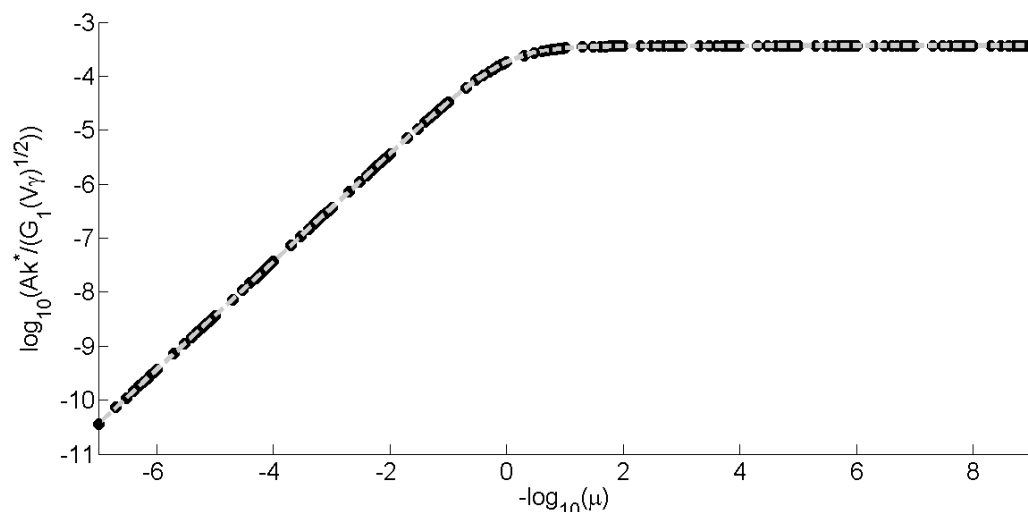


Figure 4.1: Change in viscoelastic moduli,  $R = 10\mu\text{ m}$ ,  $V = 10\text{ nm/s}$ ,  $\gamma = 1\text{ s}$  and  $\tau = 0.01\text{ s}$

Figure 4.1 is plotted by varying the viscoelastic moduli  $G_1$  and  $G_2$  in the following manner: a logarithmic scale is chosen as follows,  $[1\ 2\ 3\ 4\ 5\ 6\ 7\ 8\ 9] \times 10^a\text{ Pa}$ , that is  $a$  is varied to generate

each series, figure 4.1 was constructed with the following range of values for  $G_1$ :  $a = 2 - 10$  and the variation in  $G_2$ :  $a = 3 - 10$ . The dashed line in figure 4.1 is provided by the following equation

$$\frac{Ak^*}{G_1(V\gamma)^{1/2}} = \frac{k_1\mu}{(\mu + k_2)} \quad (4.1)$$

where  $k_1 = 3.63 \times 10^{-4}$  and  $k_2 = 0.9091$ . Equation (4.1) enables for a constant  $\tau$  (relaxation parameter) and  $\gamma$  (ramp duration) the material to be changed provided the appropriate  $k_1$  and  $k_2$  values are known. The optimal conditions can be written as,

$$\frac{Ak^*}{G_1(V\gamma)^{1/2}} = \frac{\lambda_1(\tau, \gamma)\mu}{(\mu + \lambda_2(\tau, \gamma))}$$

where  $\lambda_1(\tau, \gamma)$  and  $\lambda_2(\tau, \gamma)$  can at most be functions of  $\tau$  and  $\gamma$ .

#### 4.2 Variations in $\tau$ :

To enable the material to be changed it is necessary to determine the variation as a result of the relaxation time  $\tau$  as the variation in  $G_1$  and  $G_2$  has already been determined in equation (4.1).

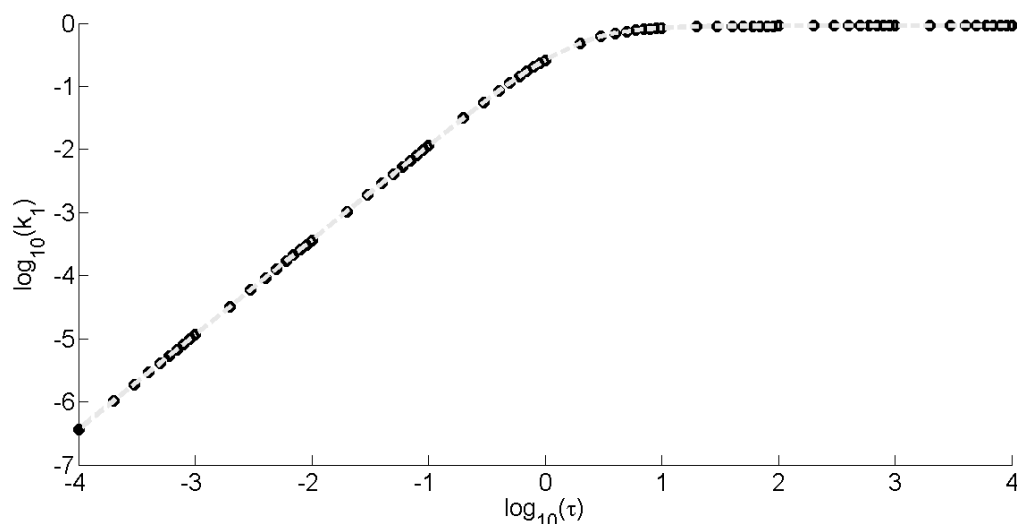


Figure 4.2: Variation in the parameter  $k_1$  as the relaxation time is varied

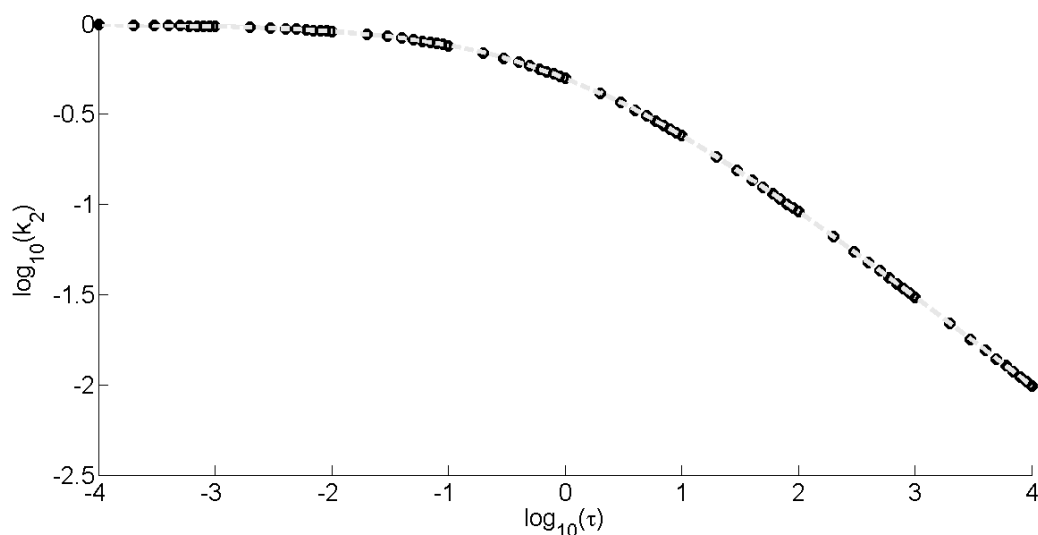


Figure 1.3: Variation in the parameter  $k_2$  as the relaxation time is varied

Figure 4.2 suggests that the functional form of  $k_1$  is,

$$k_1 = \frac{0.9091\tau^{3/2}}{\tau^{3/2} + 2.5},$$

the denominator is not dimensionally consistent and this is due to the lack of  $\gamma$  dependence; note that  $\gamma = 1$  s for the cases considered in figures 4.2 and 4.3. Figure 4.3 suggests the following functional form for  $k_2$ ,

$$k_2 = \frac{\tau^{-1/2}}{\tau^{-1/2} + 1} = \frac{1}{1 + \tau^{1/2}}.$$

A note of caution should be made here as  $\gamma$  is intricately coupled with  $\tau$  and it is unwise to assume that the full dependency on  $\tau$  is captured by fitting to these trends.

#### 4.3 Variations in $\gamma$ :

The variations in  $\gamma$  will be explored in this section.

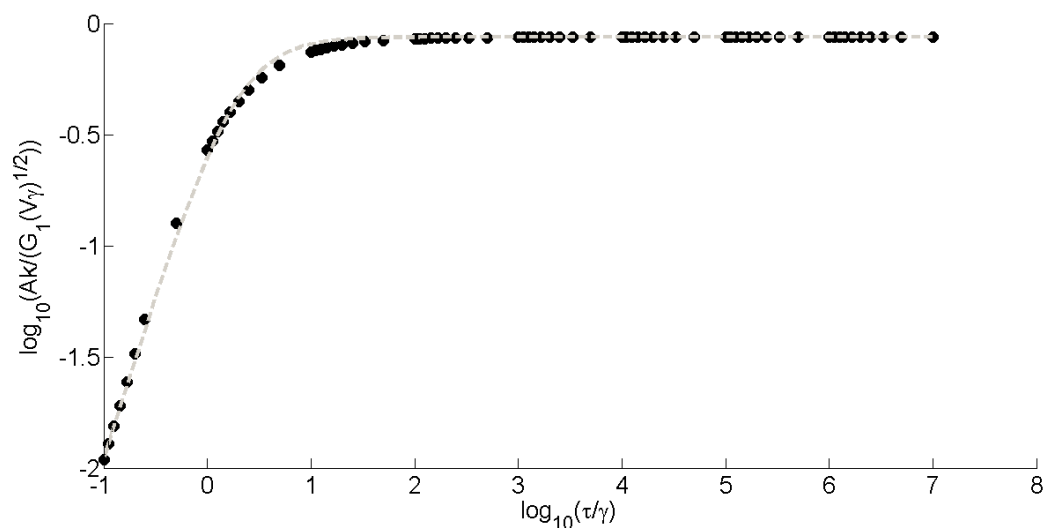


Figure 4.4: Variations in  $\gamma$  for the elastomer

The following equation is used for the approximate fit in figure 4.4,

$$\frac{Ak^*}{G_1(V\gamma)^{1/2}} = \frac{0.87\beta^{3/2}}{(\beta^{3/2} + 2.5)}$$

this suggests the following general form for the full fit,

$$\frac{Ak^*}{G_1(V\gamma)^{1/2}} = \frac{0.74\mu\beta^{3/2}}{(\mu\beta^{3/2} + 1.273)}.$$

For completeness this is linked to the parameter  $E_\infty^*$ ,

$$E_\infty^* = \frac{G_1(V\gamma)^{1/2}}{Ak^*(1 + \mu)}.$$

#### 4.4 Master curve for $h^*$ :

As with the mater curve above it is found that the important parameters are  $\mu$  and  $\beta$ .

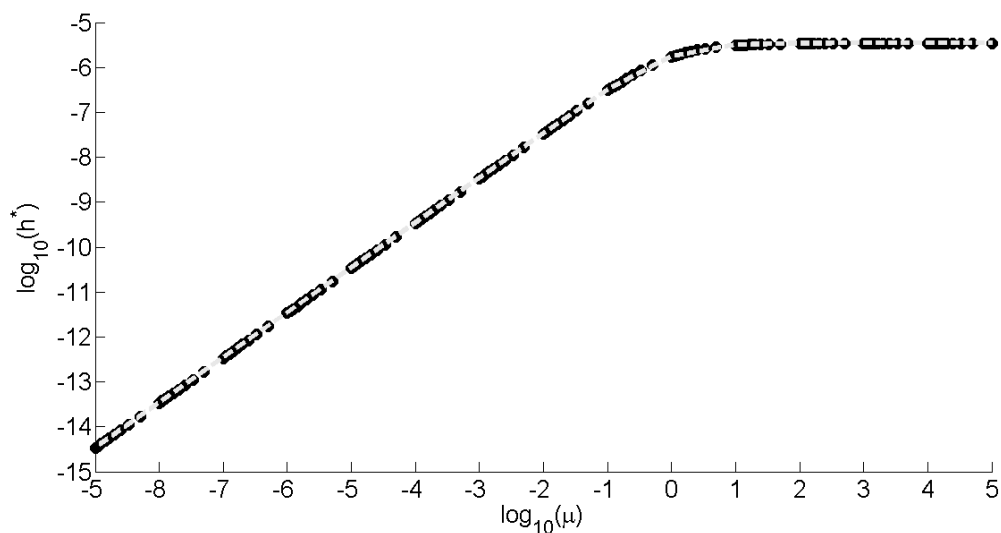


Figure 4.5: Variation in  $h^*$  with  $\mu = G_1 / G_2$ .

The dashed line in figure 4.5 is described by the following equation,

$$h^* = \frac{3.5 \times 10^{-6} \mu}{1 + \mu}.$$

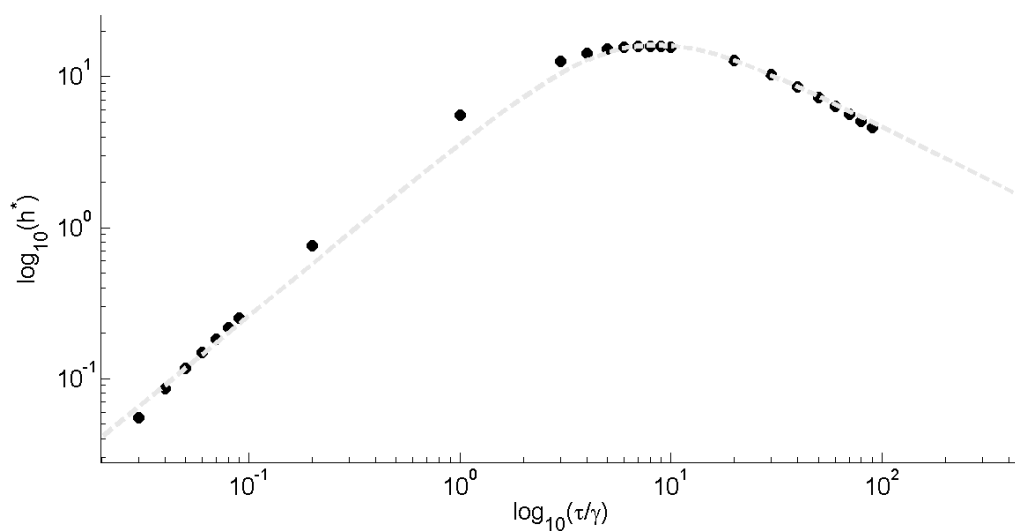


Figure 4.6: Variation in  $h^*$  with  $\beta = \tau / \gamma$ .

The dashed line in figure 4.6 is described by the following equation,

$$h^* = \frac{117\beta}{24.1 + \beta^{1.7}}.$$

This suggests the following general equation,

$$h^* = \frac{24.1\mu\beta}{24.1 + \mu\beta^{1.7}}$$

## 5. Linear programming

The equations describing the ideal parameters are obtained by further optimising the previously optimal results. The optimal results for the relative relaxation indentation depth are of a form which enables a very simple and effective approach to optimisation; here it is detailed how this may be achieved.

### 5.1: Linear programming for optimisation of parameters:

Two claims regarding the ideal parameters have been made in the manuscript, these are proven here.

1. The maximum velocity of the permissible indentation is corresponds to the ideal set of conditions
2. The ideal parameters are obtained from a simple linear programming optimisation

### 5.2: Maximum relative relaxation

It should be noted that the optimisation of parameters is simply a linear programming problem. The ideal parameters are obtained by maximising the relative relaxation,

$$\phi = V\gamma h^* \quad (5.1)$$

subject to the following constraints imposed by the method <sup>m</sup> as the maximum and minimum of the velocity, radius, spring constant and force;  $V_{\min}^m \leq V \leq V_{\max}^m$ ,  $R_{\min}^m \leq R \leq R_{\max}^m$ ,  $k_{\min}^m \leq k \leq k_{\max}^m$  and  $F_{\min}^m \leq F \leq F_{\max}^m$  respectively. The relaxation force may be written in terms of the other parameters as,

$$F = V\gamma h^* k = \frac{16h^* G_1 G_2 (V\gamma)^{3/2} (R)^{1/2}}{3E_{\infty}^* (G_1 + G_2)}. \quad (5.2)$$

As stated in the manuscript,

$$k = \frac{G_1 G_2 (V\gamma)^{1/2}}{AE_{\infty}^* (G_1 + G_2)} = \frac{16G_1 G_2 (RV\gamma)^{1/2}}{3E_{\infty}^* (G_1 + G_2)}, \text{ (note } k = k^* \text{ in the manuscript, equation (15))} \quad (5.3)$$

this enables the system to be fully described by specifying two parameters of the three unknown parameters  $(R, V, k)$  (it is assumed that the material is known and the ramp duration is fixed). The signal to noise ratio may not be great enough to measure the relaxation and hence a further constraint is required to ensure that the experiment is measurable,

$$V > V_{\min} \quad (5.4)$$

where  $V_{\min}$  is the minimum velocity for the experiment to be measurable (see manuscript equation (19)). This problem is not a linear problem; however taking logarithms allows this problem to be written as a linear programming problem. There are two possible outcomes from this optimisation, either the solution is feasible, optimal parameters exists and is bounded or the solution is infeasible and it is not possible to obtain the optimal parameters using that method (atomic force microscopy, optical tweezers, etc). For a feasible solution the ideal parameters are simply the parameter values with the largest velocity in the feasible region (the intersection of all constraints). As the solution to the linear programming problem (logarithm of equation (5.1) and all of the constraints), and since this may be written as a simple two parameter problem, it may be represented graphically and a construction may be found in (§6).

### 5.3: Linear programming construction

Taking the logarithm of the equations and boundary conditions in the above section results in the following linear programming problem; the objective function is provided by

$$\psi = \log_{10}(V\gamma h^*) \quad (5.5)$$

subject to the following constraints imposed by the method  $m$  as the maximum and minimum of the velocity, radius, spring constant and force;  $\log_{10}(V_{\min}^m) \leq \log_{10}(V) \leq \log_{10}(V_{\max}^m)$ ,  $R_{\min}^m \leq R \leq R_{\max}^m$ ,  $\log_{10}(k_{\min}^m) \leq \log_{10}(k) \leq \log_{10}(k_{\max}^m)$  and  $\log_{10}(F_{\min}^m) \leq \log_{10}(F) \leq \log_{10}(F_{\max}^m)$  respectively. The relaxation force may be written in terms of the other parameters as,

$$\log_{10}(F) = \log_{10}(V\gamma h^* k) = \log_{10}\left(\frac{16h^* G_1 G_2 (V\gamma)^{3/2} (R)^{1/2}}{3E_{\infty}^* (G_1 + G_2)}\right). \quad (5.6)$$

Equation (5.3) enables the system to be fully described by specifying two parameters of the three unknown parameters ( $\log_{10}(R), \log_{10}(V), \log_{10}(k)$ ) (it is assumed that the material is known and the ramp duration is fixed). The signal to noise ratio may not be great enough to measure the relaxation and hence a further constraint is required to ensure that the experiment is measurable,

$$\log_{10}(V) > \log_{10}(V_{\min}) . \quad (5.7)$$

This problem is a linear problem; and the ideal parameters can be obtained by the simplex method.<sup>1</sup>

### 5.4 References

- 1 D. A. Pierre, *Optimization theory with applications*, Dover, New York, 1986, ch. 5, pp. 204-209.

## 6. Construction of permissible indentation region

The construction of figures 12a) and 12b) in the manuscript are fully explained, however these figures are complicated figures and it is more illustrative to construct the figures step by step. Here a hydrogel case will be considered ( $\gamma = 10$  s) when indented by an atomic force microscopy as described in the manuscript.

### 6.1: Physical limits

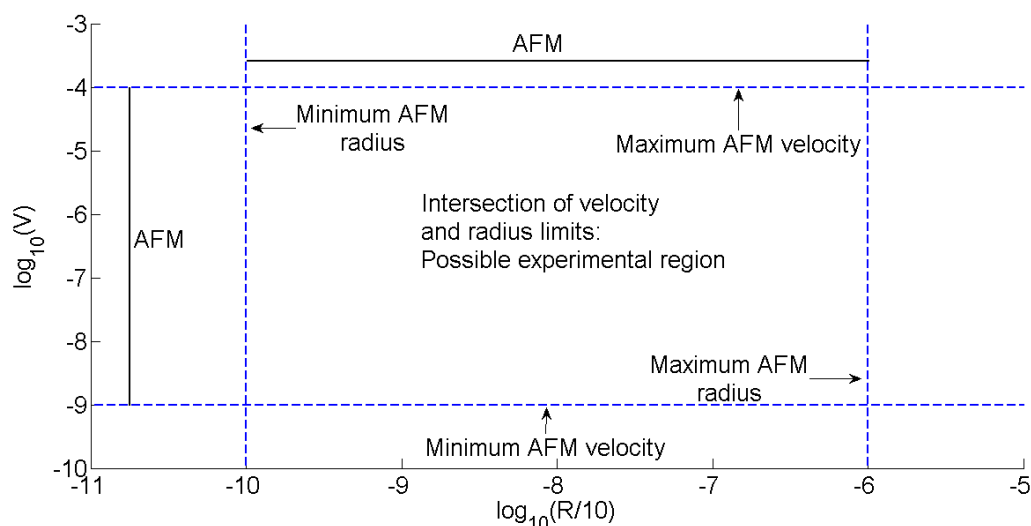


Figure 6.1: Physical limits on the radius and velocity for AFM

Figure 6.1 demonstrates the basic  $(\log(R/10), \log(V))$  parameter space; at this stage the permissible region is the intersection of the physical limits of the method.

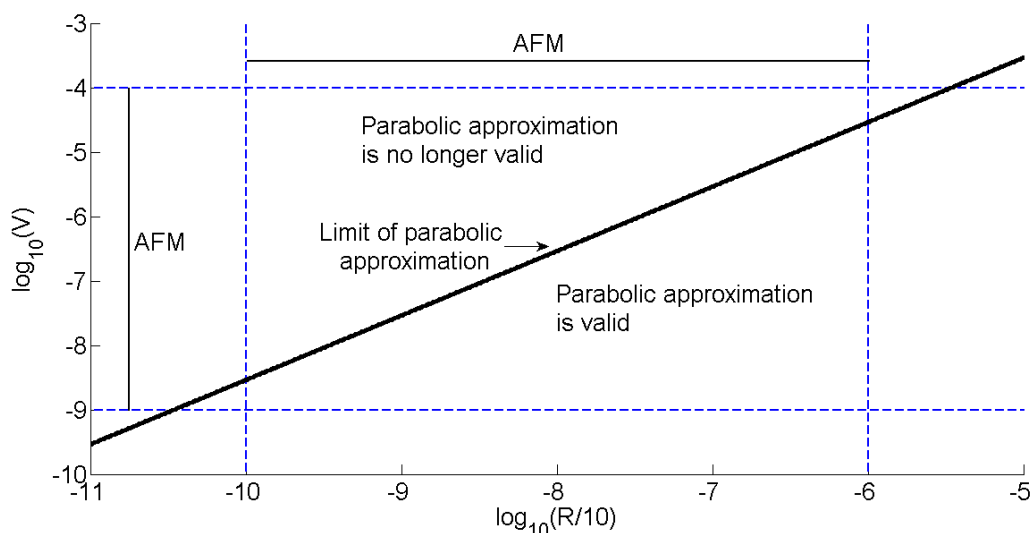


Figure 6.2: The parabolic approximation is a model limit and not a physical limit, however it results in a physical limit if the theory is to be implemented and so is included in this section. The black line represents  $h_{\max} = 0.1R$ , this imposes a maximum  $V$  for each radius.

Figure 6.2 demonstrates the limit of the parabolic approximation  $h_{\max} = 0.1R$ .

## 6.2: Calibration of spring constant axis

Figure 6.3 indicates a pre calibrated spring constant axis has been added to figure 6.2.

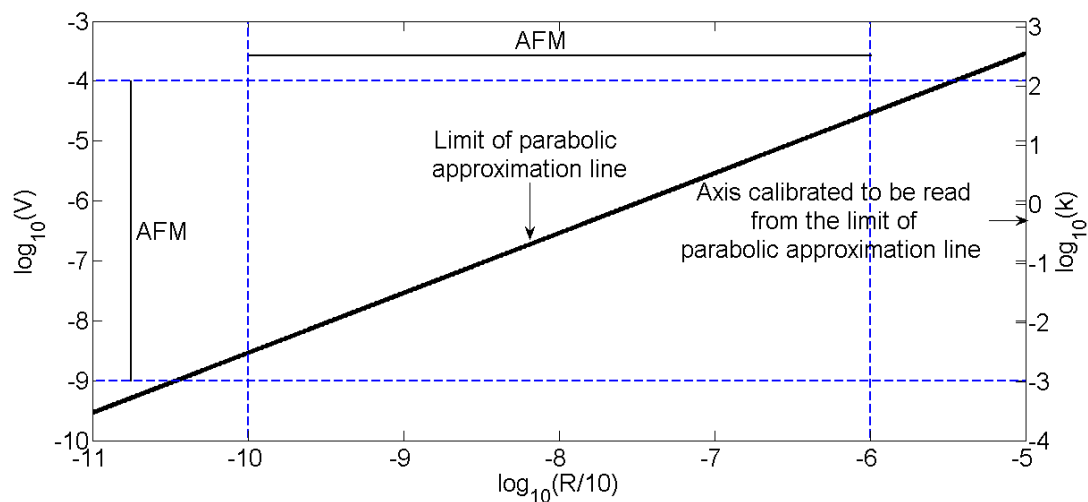


Figure 6.3: Addition of the spring constant axis

At this stage it is not possible to tell if the axis is calibrated, since no information about the spring constant has been added to the figure.

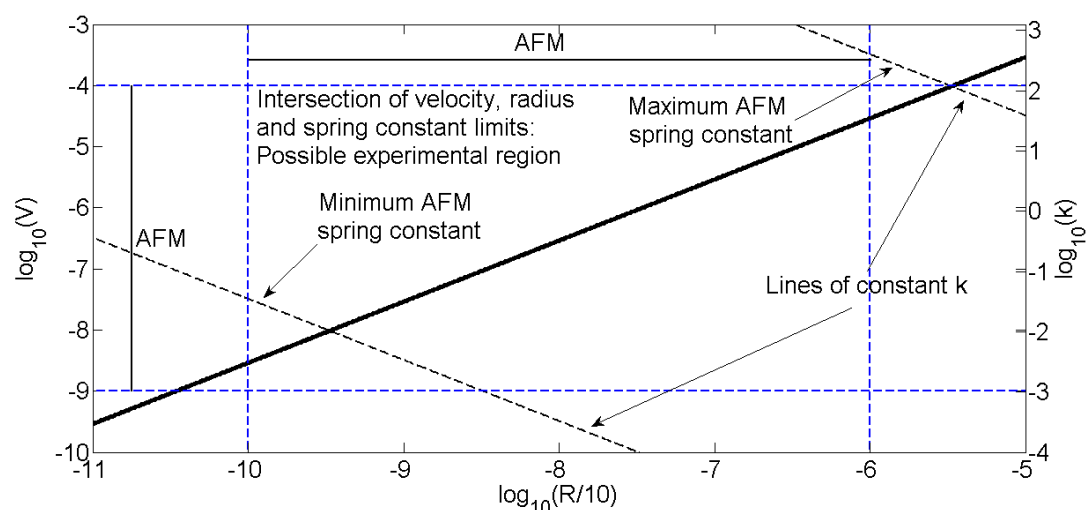


Figure 6.4: Lines of constant spring constant are plotted, in this case the limits of the currently commercially available spring stiffnesses are added these lines are used to calibrate the k axis. Equation (6.1) is used in the construction of the lines of constant k.

Figure 6.4 demonstrates how the k axis is calibrated by setting the intercept of the k limits with the limit of the parabolic line. The following equation,

$$k^* = \frac{G_1 G_2 (V\gamma)^{1/2}}{A E_\infty^* (G_1 + G_2)} = \frac{16 G_1 G_2 (R V \gamma)^{1/2}}{3 E_\infty^* (G_1 + G_2)} \quad (6.1)$$

is rearranged to determine the velocity as a function of the optimal spring constant  $k^*$  the, spring constant limits are then set equal to  $k^*$  and these are the lines of constant spring constant limits in figure 6.4. The  $k$  axis just needs to be shifted to ensure that the minimum and maximum spring constants may be read correctly at the intercept of the horizontal lines representing the  $k$  limits and the intercept of the parabolic limit line and the lines of constant  $k$  representing the  $k$  limits. Note if the velocity at the parabolic limit is used to calculate  $k^*$  the calibration of the  $k$  axis is simply obtained by shifting the  $k$  axis until the parabolic limit and the  $k^*$  line overlap.

### 6.3: Possible experimental region

Figure 6.5 reiterates that the possible experimental region is larger than the limited section permitted by the theory discussed in the manuscript. The region bounded by the green line is the possible experimental region, while only approximately half this region is permitted by the model.

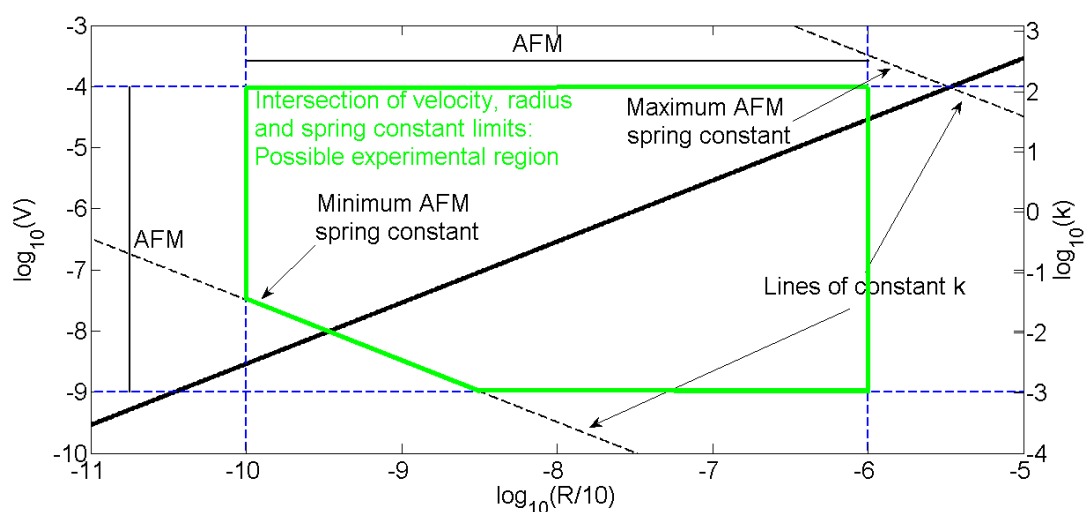


Figure 6.5: Possible experimental region, note that the force limits have not currently been applied

### 6.4: Lines of constant force

The force is provided by the following equation,

$$F = V\gamma k^* h^* \quad (6.2)$$

applying a similar approach to that detailed in step 2, the lines of constant force applied to the force limits may be added to figure 6.5 and this figure may be found in figure 6.6. Note that equation (6.2)

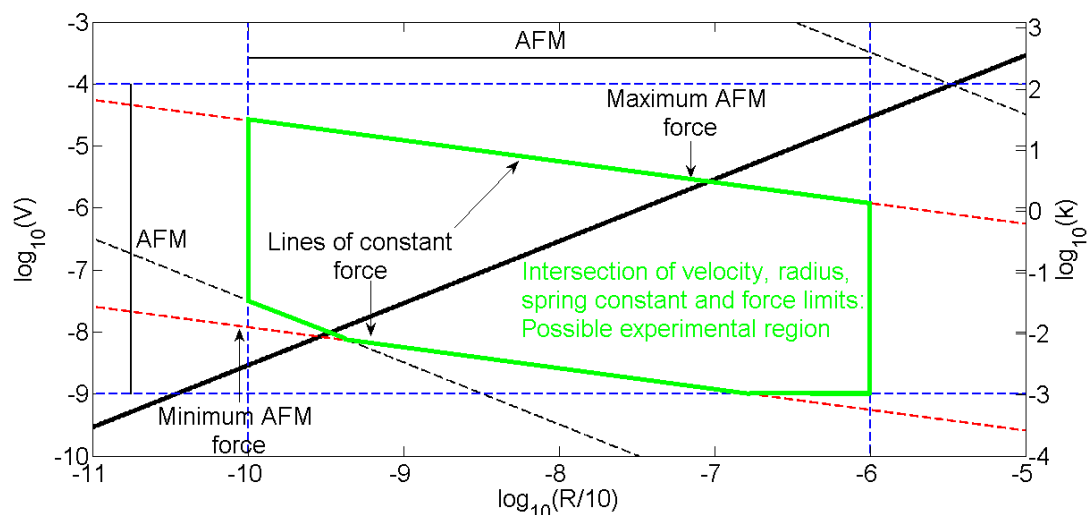


Figure 6.6: Addition of the limits of the force, lines of constant force

### 6.5: Signal to noise limit

The signal to noise limit indicates a minimum velocity required to determine the indentation from the noise. This is discussed at length in the manuscript and will not be repeated here. In this particular case this is highly restrictive and only a small region is permitted by the limits of the model and the experimental indentation method. The maximum velocity corresponds to the following ideal system parameters ( $V = 2.6394 \mu\text{m/s}$ ,  $R = 915.8 \text{ nm}$ ,  $k^* = 2.736 \text{ N/m}$ ). See figures 6.7 and 6.8, as an indication of the effect of ramp duration. Not only the permitted/possible regions are displayed in figures 6.7 and 6.8.

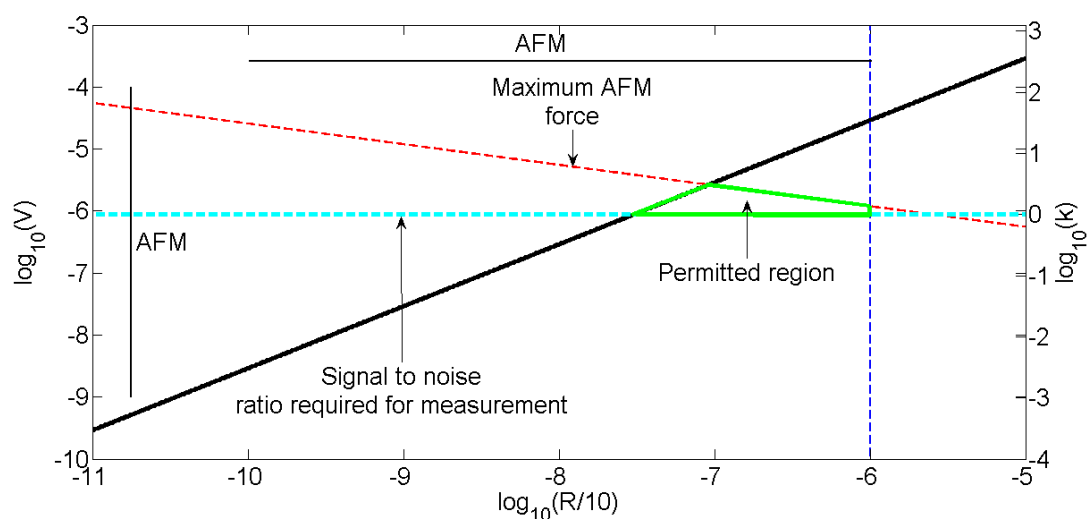


Figure 6.7: Permitted region ( $\gamma = 10 \text{ s}$ )

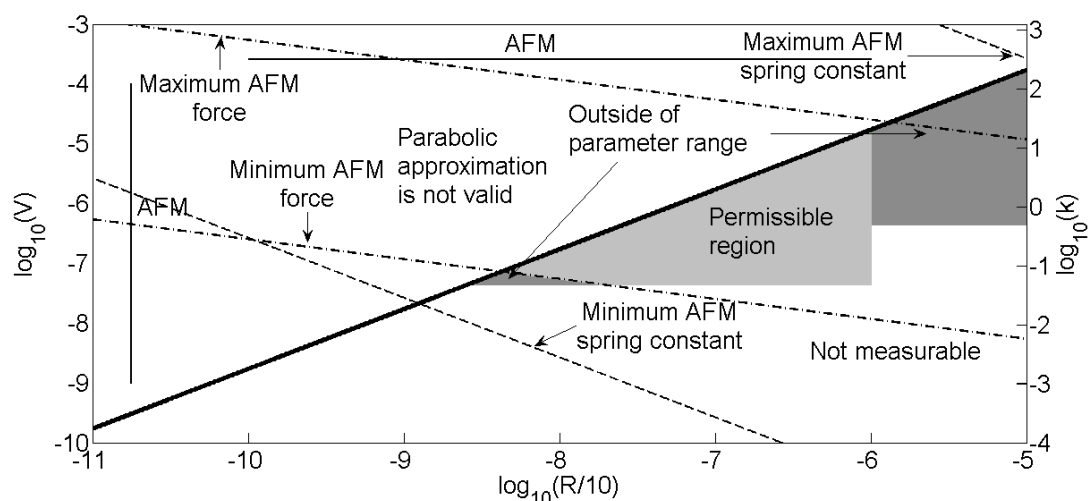


Figure 6.8: Permissible region,  $\gamma = 0.1$  s

### 6.6: Typical experimental situation:

Some notes should be made with regards to available cantilevers for AFM; cantilevers are expensive, require careful calibration, may break and it is very difficult to construct a cantilever of a specific spring constant. As such many laboratories have a range of well calibrated AFM cantilevers, if the ideal spring constant is not supplied by one of the available cantilevers it is unlikely that a new cantilever will be obtained. Provided a line of constant  $k$ , corresponding to one of the spring constants passes through the permissible region this is sufficient for the effective determination of material parameters.

## 7. Poroelasticity

A compliant poroelastic [compressible elastic matrix and incompressible fluid forming an isotropic material] problem [fixed end drive] provides the following equations for a poroelastic material<sup>1</sup>,

$$\sigma_{ij} = \alpha p \delta_{ij} = 2G \varepsilon_{ij} + \frac{2G\nu}{1-2\nu} \varepsilon_{kk} \delta_{ij} \quad (7.1)$$

$$p = \frac{2G(\nu_u - \nu)}{\alpha^2(1-2\nu_u)(1-2\nu)} (\zeta - \alpha \varepsilon_{kk}) \quad (7.2)$$

$$q_i = -\kappa p_{,i} \quad (7.3)$$

Equilibrium equations,

$$\sigma_{ij,j} = 0 \quad (7.4)$$

Continuity equations,

$$\frac{\partial \zeta}{\partial t} + q_{i,i} = 0 \quad (7.5)$$

Assuming uniaxial strain,

$$\sigma = \frac{2G(1-\nu)}{1-2\nu} \varepsilon - \alpha p, \quad (7.6)$$

the coefficient of diffusion is given by,

$$D = \frac{2\kappa G(1-\nu)(v_u - \nu)}{\alpha(1-2\nu)^2(1-\nu_u)} \quad (7.7)$$

for  $0 \leq t \leq \gamma$  the pore pressure is given by

$$\frac{\partial p_1}{\partial t} - D \frac{\partial^2 p_1}{\partial x^2} = k \left[ V - \frac{dh}{dt} \right] \frac{v_u - \nu}{\alpha(1-2\nu)(1-\nu_u)} \quad (7.8)$$

and for  $t > \gamma$

$$\frac{\partial p_2}{\partial t} - D \frac{\partial^2 p_2}{\partial x^2} = -k \frac{dh}{dt} \frac{v_u - \nu}{\alpha(1-2\nu)(1-\nu_u)} \quad (7.9)$$

the boundary conditions are provided by,

$$p(0,t) = 0, p(x,0) = 0, p_1(x,\gamma) = p_2(x,\gamma). \quad (7.10)$$

The following change of variables are invoked,

$$\tilde{t} = Dt / R^2, \tilde{x} = x / R, \tau = R^2 / D, \tilde{p} = pR / k, \tilde{h} = h / R \quad (7.11)$$

then,

$$\frac{\partial \tilde{p}_1}{\partial \tilde{t}} - \frac{\partial^2 \tilde{p}_1}{\partial \tilde{x}^2} = \left[ \tilde{V} - \frac{d\tilde{h}}{d\tilde{t}} \right] \frac{v_u - \nu}{\alpha(1-2\nu)(1-\nu_u)} \quad (7.12)$$

$$\frac{\partial \tilde{p}_2}{\partial \tilde{t}} - \frac{\partial^2 \tilde{p}_2}{\partial \tilde{x}^2} = -\frac{d\tilde{h}}{d\tilde{t}} \frac{v_u - \nu}{\alpha(1-2\nu)(1-\nu_u)} \quad (7.13)$$

The solution to equation (7.12) is,

$$\tilde{p}_1(\tilde{x}, \tilde{t}) = \int_0^{\tilde{t}} \int_0^\infty \frac{1}{\sqrt{4\pi(\tilde{t} - \tau')}} \left[ e^{-\frac{(y-\tilde{x})^2}{4(\tilde{t}-\tau')}} - e^{-\frac{(y+\tilde{x})^2}{4(\tilde{t}-\tau')}} \right] \left[ \tilde{V} - \frac{d\tilde{h}}{d\tau'} \right] \frac{v_u - \nu}{\alpha(1-2\nu)(1-\nu_u)} dy d\tau' \quad (7.14)$$

hence once the indentation depth is known as a function of time the pore pressure may be evaluated. The solution to equation (7.13) requires the solution provided in equation (7.14),

$$\begin{aligned} \tilde{p}_2 = & \int_0^{\tilde{t}-\tilde{\gamma}} \int_0^{\infty} -\frac{d\tilde{h}}{d\tau'} \frac{1}{\sqrt{4\pi(\tilde{t}-\tau')}} \left[ e^{-\frac{(y-\tilde{x})^2}{4(\tilde{t}-\tilde{\gamma}-\tau')}} - e^{-\frac{(y+\tilde{x})^2}{4(\tilde{t}-\tilde{\gamma}-\tau')}} \right] \frac{\nu_u - \nu}{\alpha(1-2\nu)(1-\nu_u)} dy d\tau' \\ & + \frac{1}{\sqrt{4\pi(\tilde{t}-\tilde{\gamma})}} \int_0^{\infty} \left[ e^{-\frac{(y-\tilde{x})^2}{4(\tilde{t}-\tilde{\gamma}-\tau')}} - e^{-\frac{(y+\tilde{x})^2}{4(\tilde{t}-\tilde{\gamma}-\tau')}} \right] \tilde{p}_1(y, \tilde{\gamma}) dy \end{aligned} \quad (7.15)$$

It should be noted at this point that if  $D$  is constant than this pressure may be written as a series of exponentials either directly or by assuming that:

$$h(t) = \sum_{i=0}^{\infty} A_i e^{\lambda_i t} \quad [\lambda_i = \text{Re}(\lambda_i) \text{ and } \lambda_i \neq \lambda_j \text{ for all } i \neq j] \quad (7.16)$$

since any differentiable function may be expressed in such a series. Given that  $h(t)$  is bounded as  $t \rightarrow \infty$ ,  $\lambda_i \leq 0$ . Now an equivalent relationship exists between the decaying exponentials series and an infinite Prony series, as such all results for the Prony series extend to poroelastic models by taking the modes which respond on the time and length scales of interest. Despite the simplicity of this approach it is valid for all bounded indentation depths even for more complicated behaviour.

## 7.1 References

- 1 O. Coussy, *Mechanics and physics of porous solids*, Wiley, 2010, ch. 4, pp. 60-75

## 8. Physical models and an equivalent viscoelastic material

Here we consider the equivalent viscoelastic material for a proposed physical model. Since the viscoelastic model can be viewed as a mathematical convenience for many materials and is open to the criticism that it ignores physical models, any equivalence between a generic physical model (deliberately left vague) and a viscoelastic material will allow the results in the manuscript to be carried over to the physical model with minimal effort. This section assumes that a proposed physical model has been solved for the problem under consideration. For example a poroelastic material is often considered, the non-dimensional indentation depth may be written in a form

similar to,  $h(t) = 1 - \sum_{n=1}^{\infty} e^{-\lambda_n t}$ , for the relaxation phase [note all the results here may be repeated for ramp phases if the series is extended to include complex error functions].

Assuming the solution to the physical model is known and takes the following form:

$$h(t) = A_0 + \sum_{n=1}^N A_n e^{-\lambda_n t}, \quad \lambda_n > 0 \quad (8.1)$$

$$\frac{dF(t)}{dt} = \sum_{l=1}^L D_l \varepsilon_l e^{-\varepsilon_l t} \quad (8.2)$$

The viscoelastic model may be written as:

$$h(t) = A_0 + B \int_0^t J(t - \xi) \frac{dF(\xi)}{d\xi} d\xi \quad (8.3)$$

Further assume that,

$$J(t) = C_0 + \sum_{k=1}^K C_k e^{-\kappa_k t}, \quad \kappa_n > 0 \quad (8.4)$$

Substituting equations (8.1), (8.2) and (8.4) into equation (8.3) and equating powers of exponents reveals,

$$-BC_0 \sum_{l=1}^L D_n (1 - e^{-\varepsilon_l t}) + \sum_{m=1}^{KL} E_m e^{-\lambda_m t} = A_n e^{-\lambda_n t} \text{ for each } n.$$

This implies that  $N = KL$  to ensure there are  $N$  equations and  $N$  unknowns. We may therefore deduce that  $L \leq N$ . Further it is hence possible to uniquely determine the parameters for an equivalent viscoelastic material where the indentation data is in perfect agreement with the physical model. It should be noted that other phenomena may not be predicted by such an approach, i.e. an equivalent viscoelastic material for a poroelastic material will not have migration of fluid but this is not required to implement the results in the manuscript. Hence there are no technical barriers to describing any physical model as an equivalent viscoelastic material for the purposes discussed in the manuscript.